

# TOWARD SHALE GAS TO LIGHT OLEFINS: AN INTEGRATED NGL RECOVERY, STEAM CRACKING, AND METHANE CONVERSION SUPERSTRUCTURE

Onur Onel\*, Alexander M. Niziolek\* and Christodoulos A. Floudas†  
Artie McFerrin Department of Chemical Engineering, Texas A&M University  
Texas A&M Energy Institute, Texas A&M University  
Department of Chemical and Biological Engineering, Princeton University

*In honor of Professor Christodoulos A. Floudas*

The authors would like to dedicate this work to Professor Floudas for his immense support and guidance during this project. His personal, professional, and academic impact will always be missed.

## *Abstract*

The growing production of natural gas liquids (NGLs) due to the recent advances in shale gas industry provides an untapped opportunity for the production of light olefins. Although olefins are currently produced by petroleum-based processes, methane and NGLs can be valuable petrochemical feedstocks for economically sustainable processes. This paper introduces a novel integrated process superstructure to recover and convert NGLs to olefins from shale gas while converting methane-rich natural gas to olefins via the methanol intermediate. In the first part, we introduce a dynamic optimization framework for an optimal ethane cracker. Then, the cracking process is integrated to the proposed superstructure through the use of a NGL recovery flowsheet. The integrated superstructure is investigated at different plant scales with different shale gas compositions. When the NGL content is high enough in the feed, NGL recovery and steam cracking is utilized in the optimal plant topology. The resulting net present values of these plants are positive at scales as low as 500 MT/day and can exceed \$5 billion at scales as high as 5000 MT/day.

## *Keywords*

Shale gas, steam cracking, NGL recovery, process synthesis, olefins

## **Introduction**

Decreased prices of natural gas coupled with the growing production of natural gas liquids, such as ethane, propane, and butane, provide an untapped opportunity for producing olefins from shale gas (Floudas et al., 2016). In some wet shale plays, NGL fraction can exceed 30% (Hill et al., 2007). Previous work has already shown methane rich natural gas as a viable and profitable alternative to produce light olefins including ethylene, propylene, and butene isomers (Onel et al., 2016). However, growing NGLs

production has enabled recent industrial efforts to build new ethane crackers for an annual combined capacity of 12.5 million tonnes in the United States (Chang, 2014). Hence, inexpensive shale gas can be converted into high value olefins through an integrated NGL recovery, steam cracking, and methane conversion process.

The integrated approach first requires the efficient recovery of NGLs from the shale gas feed (Luyben, 2013). Then, these liquids can be thermally or catalytically cracked

---

\* To whom all correspondence should be addressed: [onel@princeton.edu](mailto:onel@princeton.edu), [niziolek@princeton.edu](mailto:niziolek@princeton.edu)

to yield high value olefins (Onel et al., 2016, Sundaram and Froment, 1977). Subsequently, the methane rich dry gas can be converted into olefins with high selectivity (Onel et al., 2016). Within this approach, steam-cracking reactor is of major importance, since it involves non-intuitive decision variables (feed amount, residence time, steam-to-hydrocarbon ratio, heat flux profile) along with significant trade-offs (hydrocarbon conversion, olefin yield, coking). Moreover, the existence of novel and competing process alternatives necessitates the synthesis and global optimization of such processes through using an extensive process superstructure (Niziolek et al., 2016, Onel et al., 2015, 2016).

In this work, we present a dynamic optimization framework to optimize the configuration of a steam cracking reactor subject to feedstock amounts, steam-to-hydrocarbon ratio, and heat flux profile while maximizing the operating profit of the reactor. Subsequently, the optimal steam cracker is, for the first time, implemented into a process superstructure that integrates NGLs recovery, steam cracking, and methane conversion alternatives. The case studies will quantify the economic benefit of shale gas to olefins processes across different gas compositions using this integrated process. The paper continues with (i) ethane cracking modeling & optimization, (ii) shale gas to olefins superstructure, (iii) computational case studies, and (iv) conclusions.

### Steam Cracking of Ethane: Modeling & Optimization

The steam cracking process is a non-catalytic process that thermally cracks paraffinic hydrocarbons into olefins and byproducts (e.g., aromatics, pyrolysis gasoline). Although the kinetics for ethane cracking and coking are well established (Sundaram and Froment, 1977a, Sundaram et al., 1981), naphtha is mainly used in industry in steam cracking applications. The growing production of NGLs is an opportunity to investigate optimal ethane cracking reactors since ethane cracking yields a higher ethylene fraction and requires less investment compared to naphtha cracking.

We first dynamically modeled the ethane cracking reactor using 15 underlying equations and their Arrhenius type kinetics reported in the literature (Sundaram and Froment, 1977a, 1977b, Kumar and Kunzru, 1985), where the dynamic behavior is caused by coking and is handled by quasi-steady state approximation. The underlying ODEs for simulating the reactor are:

$$\frac{dF_j}{dz} = -\left(\sum s_{ij}r_i\right)\frac{\pi D_t^2}{4} \quad \forall j \quad (1)$$

$$\frac{dT}{dz} = \frac{\left[Q(z)\pi D_t + \frac{\pi D_t^2}{4}\sum r_i(-\Delta H)_i\right]}{\sum F_j C_{pj}} \quad (2)$$

$$\frac{dp_t}{dz} = \frac{\frac{d}{dz}\left(\frac{1}{M_m}\right) + \frac{1}{M_m}\left(\frac{1}{T}\frac{dT}{dz} + Fr\right)}{\frac{1}{M_m p_t} - \frac{p_t}{G^2 RT}} \quad (3)$$

where  $j$  represents the species,  $i$  represents the reactions,  $z$  is the reactor spatial coordinate,  $F$  represents the molar flow rates,  $s$  represents the stoichiometric coefficients,  $r$  represents the reaction rates,  $Q$  is the external heat flux,  $M_m$  is the mean molecular weight,  $Fr$  is the friction factor,  $T$  represents temperature,  $p_t$  represents pressure,  $D_t$  is the tube diameter,  $\Delta H_i$  is the heat of reaction, and  $G$  is the total mass flow rate. The boundary condition  $F_j(z=0) = F_{j,o}$  specifies the inlet flowrates. The model and kinetics are validated through simulating the aforementioned model and comparison of the results with industrial data. Then, we discretized the model to enable mathematical optimization, via converting ODEs into nonlinear constraints.

### Discretization via Orthogonal Collocation

The model is discretized using orthogonal collocation on finite elements, which is a well-established method to convert ODEs into a set of non-linear equalities (Cutthrell and Biegler, 1987). The discretization is based on estimating the state variables and controlled variables using piecewise Lagrange interpolating polynomials:

$$F_n^{K+1}(z) = \sum_{i=0}^K \hat{F}_{n,i} \phi_{n,i}(z) \quad (4)$$

$$\phi_{n,i}(z) = \prod_{k=0, k \neq i}^K \frac{z - z_{n,k}}{z_{n,i} - z_{n,k}} \quad (5)$$

$$U_n^K(z) = \sum_{i=1}^K \hat{U}_{n,i}(z) \psi_{n,i}(z) \quad (6)$$

$$\psi_{n,i}(z) = \prod_{k=1, k \neq i}^K \frac{z - z_{n,k}}{z_{n,i} - z_{n,k}} \quad (7)$$

where  $n$  represents the finite elements,  $i$  represents the collocation points,  $F$  represents the state variables,  $U$  represents the controlled variables, and  $\phi$  and  $\psi$  represent the basis functions. The polynomials are substituted in the original differential equation and matched at the collocation points at each finite element, creating as many equality constraints as discretizations. Finally, continuity between finite elements are introduced as equality constraints as well. Eventually, each ODE can be replaced with  $(K+1)N-1$  equality constraints where  $K$  is the number of collocation points and  $N$  is the number of finite elements.

### Modeling of Coke Formation

Coke formation is one of the major challenges for the operation of an ethane cracker (Sundaram et al., 1981). The formation of coke needs to be accurately modeled to represent the operational time of the reactor as well as downtime during decoking cycles. Coking is modeled with a quasi-steady state approximation, since the coking rate is significantly slower than the cracking rate. Within this approximation, the diameter is updated after each time step and model is solved at steady state between each time step. The kinetics of coking are represented as:

$$\Delta d_c = \frac{A_o \exp\left(-\frac{E_a}{RT}\right) \bar{C} \Delta t}{\rho_c \cdot 10^6} \quad (8)$$

$$d_{t,new} = d_{t,old} - 2\Delta d_c \quad (9)$$

where the thickness of coke ( $\Delta d_c$ ) is a function of kinetic parameters (Sundaram et al., 1981), average mass concentration of  $C_{4+}$  species ( $\bar{C}$ ), and the density of coke ( $\rho_c$ ). The diameter is updated using equation 9 at each time step. It should be noted that the policy rule for decoking is such that the reactor is shut down for 48 hours after the diameter is reduced by 25% at any point within the reactor.

### Ethane Cracking Optimization Model

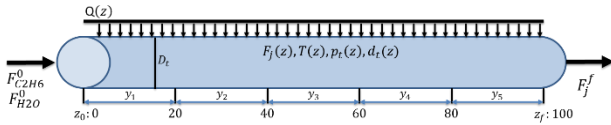


Figure 1. Ethane cracking tubular reactor

The objective function of the reactor optimization model maximizes the profit subject to the inlet ethane flow rate, steam flow rate, heat flux profile, and the reactor length.

$$MAX \text{ Revenue} - C_{Feed} - C_Q - C_{Inv} - C_{Decoke} \quad (10)$$

The inlet steam-to-ethane ratio is constrained to be between 0.33 – 1.70. The temperature within any point of the reactor is constrained not to exceed 1300K due to metallurgical reasons, whereas the lower bound on pressure is 1 bar. The following cost parameters are used for the optimization model:

Table 1. Cost Parameters for Ethane Cracking Optimization Model

| Parameter                 | Cost                   |
|---------------------------|------------------------|
| Ethane                    | \$0.3/kg               |
| Ethylene                  | \$1.382/kg             |
| Steam                     | \$0.0129/kg            |
| Heat                      | \$1.26E-8/J            |
| Levelized Tube Investment | \$0.00545/piece/s      |
| Decoking                  | \$66000/decoking cycle |

The model is discretized with 5 finite elements and 5 collocation points using the roots of the Shifted Legendre Polynomial. Overall, the model has 2305 variables, 1875 constraints, and 4 binary variables (that represent the reactor tube pieces). Since the commercial global solvers cannot solve the model due to stiffness, the resulting non-convex mixed-integer nonlinear problem (MINLP) is solved using DICOPT (Grossmann et al., 2002) using a multi-start approach to generate a diverse set of local solutions and the best solution is selected. It should be noted that the optimal reactor length is selected to be 40 meters (2 pieces), since

high conversions are achieved early on and a shorter reactor ensures limited synthesis of byproducts. The detailed results on the optimization are shown on Tables 2 and 3.

Table 2. Ethane Cracking Optimization Results (Bold denotes decision variables)

| Variable                               | Value         |
|--|---------------|
| <b>Inlet Ethane (kmol/s)</b>           | <b>0.0294</b> |
| <b>Inlet Steam (kmol/s)</b>            | <b>0.0215</b> |
| <b>Q<sub>1</sub>(MW/m<sup>2</sup>)</b> | <b>0.03</b>   |
| <b>Q<sub>2</sub>(MW/m<sup>2</sup>)</b> | <b>0.67</b>   |
| Ethane Conversion                      | 0.8202        |
| Ethylene Selectivity                   | 0.9086        |
| Ethylene Yield                         | 0.7453        |
| Runtime (hrs)                          | 361.28        |
| T <sub>out</sub> (K)                   | 1245          |
| P <sub>out</sub> (bar)                 | 1             |

Table 3. Ethane Cracking Objective Variables

| Variable                | Value (\$/s) |
|-------------------------|--------------|
| Ethane                  | -0.2342      |
| Steam                   | -0.0044      |
| Heat                    | -0.0526      |
| Investment              | -0.0109      |
| Decoking                | -0.0448      |
| Ethylene                | 0.7501       |
| Profit                  | 0.4031       |
| <b>Profit (MM\$/yr)</b> | <b>11.61</b> |

As a result, a significantly profitable cracking reactor can be configured using the above methodology. Since the underlying dynamic model is stiff and non-linear the dynamically optimized ethane cracker is used to generate a stoichiometric model which is implemented into the superstructure along with a NGL recovery process.

### An Integrated Superstructure for Shale Gas to Olefins: NGL Recovery, Steam Cracking, and Methane Conversion

Previous work has shown that methane rich natural gas can effectively be converted into olefins with high selectivity (Onel et al., 2016). This study builds upon that by exploiting the untapped potential of recovering the NGLs and further converting them into olefins.

#### Natural gas liquids recovery and ethane cracking

The NGLs rich natural gas is first sent to the demethanizer column to separate methane and NGLs. The methane is directed to the natural gas conversion section, whereas NGLs are directed to a series of distillation columns for further separation. Deethanizer recovers ethane at the top and higher NGLs at the bottom. Ethane is mixed with the recycled ethane and directed to the cracking reactor along with steam. The cracked gas is further fractionated to

separate wastewater, pyrolysis gasoline, and light gases and the olefin mixture is sent to the olefin purification section.

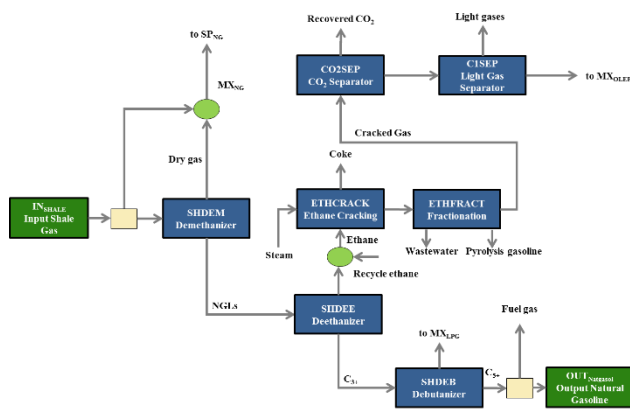


Figure 2. NGL recovery section

The remaining NGL mixture is sent to a distillation column to separate propane and butane from higher hydrocarbons. Higher hydrocarbons are either output as natural gasoline or utilized as fuel gas within the refinery. The propane-butane mixture is sent to the LPG processing for further upgrading.

#### Methane conversion and syngas cleaning

Methane rich natural gas can be reformed via autothermal reforming or steam reforming process to produce raw syngas or converted directly to methanol via partial oxidation. The steam reformer and the autothermal reformer operate at discrete temperatures and facilitate the steam methane reforming and water-gas shift reactions toward equilibrium. Partial oxidation process catalytically converts natural gas with a per-pass conversion of 13%.

The raw syngas produced from the reformers is treated in the syngas cleaning section. First, an optional water gas shift reactor adjusts the  $H_2/CO$  ratio. Then, syngas is cooled and flashed to remove the water. Dry syngas is then sent to an optional  $CO_2$  recovery unit. The captured  $CO_2$  can be vented, sequestered, or recycled back within the refinery depending on the environmental constraints imposed within the refinery. The dry and  $CO_2$ -lean syngas is sent to the methanol synthesis section.

#### Methanol synthesis and conversion

The syngas is sent to the methanol synthesis reactor that operates at  $250^\circ C$  and 45 bar and directs the methanol synthesis and water gas shift reactions toward equilibrium. The raw methanol is flashed to recycle back unreacted syngas and is further degassed to remove entrained gases within the methanol-water mixture. The methanol is then directed to one of the two conversion alternatives: methanol-to-olefins (MTO) and methanol-to-propylene (MTP). MTO reactor utilizes a SAPO-34 catalyst to efficiently convert methanol into an olefin mixture (>95% selectivity). The reactor operates at  $375^\circ C$  and 1 bar and

produces ethylene, propylene, and butenes (Mokrani and Scurrill, 2009). MTP reactor utilizes a ZSM-5 based proprietary catalyst to boost the propylene selectivity. The process operates at  $425^\circ C$  and 1.5 bar (Rothamel and Holtmann, 2002). All of the methanol is converted to produce mainly propylene (71.37%) and by-product gasoline (19.85%). The effluents of both reactors are fractionated and the olefin mixture is sent to the olefin purification section, whereas gasoline is obtained as byproduct and water is directed to the wastewater treatment section.

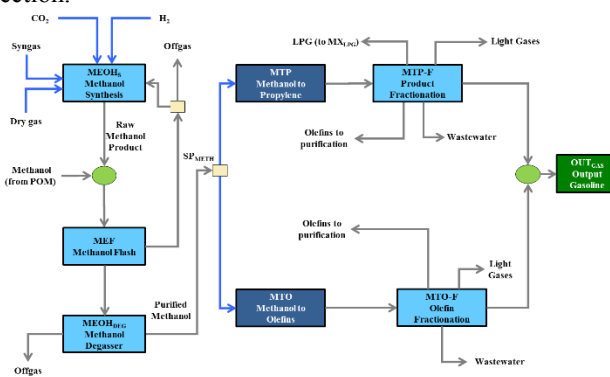


Figure 3. Methanol synthesis and conversion

#### LPG processing

LPG can be output as a product or further dehydrogenated to increase olefin selectivity. First, a debutanizer distillation column separates  $C_3$  hydrocarbons from  $C_4$  hydrocarbons (Onel et al., 2016). The distillate is directed to one of the two catalytic dehydrogenation processes ( $C_3$  Catofin or  $C_3$  Oleflex) to produce propylene product. The bottom from the debutanizer is first sent to the UOP Butamer process (Meyers, 2004) to convert n-butane to isobutane. Isobutane stream is split to one of the two catalytic dehydrogenation processes ( $C_4$  Catofin or  $C_4$  Oleflex) to produce isobutylene product.

#### Olefin purification section

The olefins produced via steam cracking, MTO, and MTP processes are purified to product quality in this section. First, steam cracking and MTO effluent is directed to a deethanizer column to recover  $C_2$  stream in the distillate (Onel et al., 2016). This stream is directed to a selective hydrogenation process to convert acetylenes and then sent to a  $C_2$  distillation column to recover ethylene as a product.

The deethanizer bottom that contains  $C_3$  and  $C_4$  hydrocarbons is mixed with the MTP effluent and directed to the depropanizer column to separate  $C_3$  and  $C_4$  hydrocarbons.  $C_3$  hydrocarbons are further separated in a distillation column to recover propylene as a product (Onel et al., 2016).

The depropanizer bottom that contains a butane-butene mixture is directed to a dimethylformamide based extractive distillation column. The butanes are recycled back within

the process whereas the butenes can be (i) output as a crude mixture, (ii) cracked in the Olefin Cracking Process to produce ethylene & propylene (Chen et al., 2005), (iii) separated to 1-butene and 2-butene in a distillation column, or (iv) oxidatively dehydrogenated to produce butadiene (Crone et al., 2009).

### Utility Plants

The superstructure also incorporates multiple alternatives for hydrogen and oxygen production as well as light gas recycle (Onel et al., 2016). Simultaneous heat, power, and water integration (Elia et al., 2010) ensures minimal usage of external utility and maximum utilization of waste heat within the refinery.

### Mathematical model and objective function

The objective function of the model aims to maximize the profit of olefin production while taking into account the feedstock, electricity, sequestration, and leveled investment costs along with product revenues.

$$MIN \sum_{f \in F} C^f + C^{El} + C^{Seq} + \sum_{u \in U_I} C_u^U - \sum_{p \in P} C^p \quad (11)$$

The overall model has 21,873 continuous variables, 30 binary variables, 26,846 constraints, and 570 non-convex terms (bilinear, trilinear, quadrilinear, and concave). This large scale non-convex model is solved to global optimality using a branch-and-bound global optimization framework. The lower bounding problem is generated by using piecewise linear & McCormick underestimators to generate a MILP. The upper bounding problem is an NLP for which the binary variables are fixed from the MILP (Baliban et al., 2012). The optimality gap is reduced significantly (<5%) within a branch-and-bound framework to provide globally optimal process designs in 100 hours.

### Computational Studies

The integrated process superstructure is used to investigate two different shale gas compositions (see Table 4) at two different plant scales (500 and 5000 MT/day). Different shale gas compositions are investigated to observe the relative benefit of the integrated superstructure across different feeds. Different plant scales are investigated to evaluate economies of scale and plant profitability. Case studies are denoted as W[N]-[M] where N represents the well number and M represents the plant capacity in MT/day.

Optimal process topologies are presented in Table 5. In most case studies ethane cracking is utilized in the optimal topology along with NGL recovery. This signifies that the integrated process can exploit an opportunity for increasing the profit through the steam cracking route. Since the ethane composition is smaller in the second well composition, ethane cracking process is not utilized at the small scale due to the economies of scale. The Oleflex process is consistently utilized for dehydrogenation of C<sub>3</sub> and C<sub>4</sub>

hydrocarbons. Methane is converted to olefins through ATR and MTO processes, which is consistent with the previous findings (Onel et al., 2016). CO<sub>2</sub> sequestration is only required for the first well composition, since the higher overall carbon conversion in the second well composition negates the need for sequestration to meet the life-cycle emission constraint.

Table 4. Well compositions (Hill et al., 2007)

| Species                          | Texas Well 1 | Texas Well 2 |
|----------------------------------|--------------|--------------|
| N <sub>2</sub>                   | 2.582        | 2.857        |
| Ar                               | 0.484        | 0.181        |
| CO <sub>2</sub>                  | 0.787        | 0.511        |
| CH <sub>4</sub>                  | 54.610       | 77.943       |
| C <sub>2</sub> H <sub>6</sub>    | 15.634       | 8.903        |
| C <sub>3</sub> H <sub>8</sub>    | 15.564       | 5.534        |
| n-C <sub>4</sub> H <sub>10</sub> | 4.811        | 2.236        |
| i-C <sub>4</sub> H <sub>10</sub> | 2.542        | 1.063        |
| n-C <sub>5</sub> H <sub>12</sub> | 1.575        | 0.411        |
| i-C <sub>5</sub> H <sub>12</sub> | 1.411        | 0.361        |

Table 5. Optimal Process Topologies

| Topology             | W1-500  | W1-5000 | W2-500 | W2-5000 |
|----------------------|---------|---------|--------|---------|
| Eth. Cracking        | Y       | Y       | -      | Y       |
| Methane Conv.        | ATR     | ATR     | ATR    | ATR     |
| MTO                  | Y       | Y       | Y      | Y       |
| MTP                  | -       | -       | -      | -       |
| C3-Dehyd.            | Oleflex | Oleflex | -      | Oleflex |
| C4-Dehyd.            | Oleflex | Oleflex | -      | Oleflex |
| Butene Dist.         | Y       | Y       | Y      | Y       |
| Oxo-D                | -       | -       | -      | -       |
| CO <sub>2</sub> -Seq | Y       | Y       | -      | -       |
| GT                   | -       | -       | -      | -       |

Table 6. Overall Cost & Revenue Breakdown

| Cost (\$/GJ)         | W1-500 | W1-5000 | W2-500 | W2-5000 |
|----------------------|--------|---------|--------|---------|
| Shale gas            | 6.16   | 6.39    | 7.23   | 6.57    |
| Water                | 0.01   | 0.01    | 0.01   | 0.00    |
| Investment           | 7.14   | 3.25    | 7.25   | 3.44    |
| CO <sub>2</sub> Seq. | 0.02   | 0.04    | 0.00   | 0.00    |
| O&M                  | 1.89   | 0.86    | 1.91   | 0.91    |
| Electricity.         | 1.57   | 1.27    | 0.63   | 1.11    |
| Gasoline             | -0.37  | -0.32   | -0.71  | -0.48   |
| LPG                  | -0.10  | -0.09   | -0.17  | -0.12   |
| Nat. Gasoline        | 0.00   | 0.00    | 0.00   | 0.00    |
| Ethylene             | -8.30  | -8.09   | -9.67  | -9.42   |
| Propylene            | -13.83 | -13.86  | -13.69 | -13.01  |
| i-Butene             | -4.69  | -5.39   | 0.00   | -3.27   |
| 1-Butene             | -3.05  | -2.65   | -5.72  | -3.93   |
| 2-Butene             | -0.44  | -0.38   | -0.86  | -0.58   |
| Mixed Butene         | 0      | 0       | 0      | 0       |
| Butadiene            | 0      | 0       | 0      | 0       |

|               |        |        |        |        |
|---------------|--------|--------|--------|--------|
| Total (\$/GJ) | -14.00 | -18.97 | -13.77 | -18.78 |
| NPV (MM\$)    | 283    | 5956   | 271    | 5839   |

The overall cost breakdown is presented in Table 6. Significant reductions on levelized investment costs are observed when plant scale is increased from 500 MT/day to 5000 MT/day. A majority of the revenue is obtained from the sales of olefin products, whereas byproduct gasoline and LPG make up a small contribution. For a scale of 500 MT/day, profits range between \$13.77/GJ and \$14.00/GJ. When the scale is increased to 5000 MT/day, the profits range between \$18.78/GJ and \$18.97/GJ. Due to the scaling effects the net present value exceeds \$5 billion for the large scale case studies. Even at lower scales, positive net present values (>271MM\$) can be observed through this integrated process.

## Conclusions

This paper introduced an integrated framework toward the production of light olefins using NGL-rich shale gas reserves. The untapped opportunities regarding NGL recovery and ethane cracking are utilized within the natural gas based olefins refinery.

Since the ethane cracking process has well established kinetics, dynamic optimization techniques are used to propose a reactor design with optimal inlet conditions, heat flux, and reactor length. The optimization model also considered coking and decoking cycles within its operation.

The optimal ethane cracker is integrated to a shale gas to olefins superstructure along with an NGL recovery process. The NGL recovery process utilizes a series of distillation columns to separate different cuts of the natural gas feed and direct them to the necessary parts of the superstructure. The extensive superstructure resulted in a large-scale nonconvex MINLP model that is solved to global optimality using a branch-and-bound framework.

The case studies across different shale gas compositions has shown that the integrated process has significant potential to increase the plant profitability and exploit the opportunity to utilize the growing production of natural gas liquids. The use of different plant scales showed the potential gains through economies of scale when larger scale plants are considered. Overall, significant plant profitability is observed with positive NPVs.

## Acknowledgments

The authors acknowledge partial financial support from National Science Foundation (NSF EFRI-0937706 and NSF CBET-1158849).

## References

Baliban, R.C., Elia, J. A., Misener, R., Floudas, C. A. (2012). Global Optimization of a MINLP Process Synthesis Model for Thermochemical Based Conversion of Hybrid Coal, Biomass, and Natural Gas to Liquid Fuels. *Comp. Chem. Eng.*, 42, 64-86.

Chang, J. (2014). New projects may raise US ethylene capacity by 52%, PE by 47%, *ICIS Petrochemicals*.

Chen, J. Q., Bozzano, A., Glover, B., Fuglerud, T., Kvisle, S. (2005). Recent advancements in ethylene and propylene production using the UOP/Hydro MTO process. *Catal. Today*, 106, 103-107.

Crone, S., Klanner, C., Schindler, G. P., Duda, M., Borgmeier, F. (2009). Method for producing butadiene from n-butane, US Patent 5,288,370.

Cuthrell, J. E., Biegler, L. T. (1987). On the optimization of differential-algebraic process systems, *AIChE J.*, 33(8), 1257-1270.

Elia, J. A., Baliban, R. C., Floudas, C. A. (2010). Toward Novel Biomass, Coal, and Natural Gas Processes for Satisfying Current Transportation Fuel Demands, 2: Simultaneous Heat and Power Integration. *Ind. Eng. Chem. Res.*, 49, 7371-7388.

Floudas, C. A., Niziolek, A. M., Onel, O., Matthews, L. R. (2016). Multi-scale systems engineering for energy and the environment: Challenges and opportunities. *AIChE J.*, 62(3), 602-623.

Grossmann, I. E., Viswanathan, J., Vecchietti, A., Raman, R., Kalvelagen, E. (2002). GAMS/DICOPT: A discrete continuous optimization package. GAMS Development Corporation, Washington, DC.

Hill, R. J., Jarvie, D. M., Zumberge, J., Henry, M., Pollastro, R. M. (2007). Oil and gas geochemistry and petroleum systems of the Fort Worth Basin, *AAPG Bulletin*, 91(4), 445-473.

Kumar, P., Kunzru, D. (1985). Modeling of naphtha pyrolysis, *Ind. Eng. Chem. Process Des. Dev.*, 24, 774-782.

Luyben, W. L. (2013). NGL Demethanizer Control, *Ind. Eng. Chem. Res.*, 52, 11626-11638.

Meyers, R. A. (2004). Handbook of Petroleum Refining Processes, *McGraw-Hill*, New York, Vol 3.

Mokrani, T., Scurrall, M. (2009). Gas Conversion to Liquid Fuels and Chemicals: The Methanol Route – Catalysis and Process Development, *Catal. Rev. Sci. Eng.*, 51, 1-145.

Niziolek, A. M., Onel, O., Floudas, C. A. (2016). Production of benzene, toluene, and xylenes from natural gas via methanol: Process synthesis and global optimization, *AIChE Journal*, 62(5), 1531-1556.

Onel, O., Niziolek, A. M., Elia, J. A., Baliban, R. C., Floudas, C. A. (2015). Biomass and Natural Gas to Liquid Transportation Fuels and Olefins (BGTL+C2\_C4): Process Synthesis and Global Optimization, *Ind. Eng. Chem. Res.*, 54(1), 359-385.

Onel, O., Niziolek, A. M., Floudas, C. A. (2016). Optimal Production of Light Olefins from Natural Gas via the Methanol Intermediate, *Ind. Eng. Chem. Res.*, 55(11), 3043-3063.

Rothaemel, M., Holtmann, H. D. (2002). Methanol to propylene MTP: Lurgi's way. *Erdol, Erdgas, Kohle*, 118, 234-237.

Sundaram, K. M., Froment, G. F., (1977a). Modeling of thermal cracking kinetics – I: Thermal cracking of ethane, propane and their mixtures, *Chem. Eng. Sci.*, 32(6), 601-608.

Sundaram, K. M., Froment, G. F., (1977b). Modeling of thermal cracking kinetics – II: Thermal cracking of iso-butane, of n-butane and of mixtures ethane-propane-n-butane, *Chem. Eng. Sci.*, 32(6), 609-617.

Sundaram, K. M., Van Damme, P. S., Froment, G. F. (1981). Coke Deposition in the Thermal Cracking of Ethane, *AIChE Journal*, 27(6), 946-951.